

## Electronic Structure of Metallacycloposphazene and Metallacyclothiazene Complexes

Andreas Sundermann and Wolfgang W. Schoeller\*

Fakultät für Chemie, Universität Bielefeld, Postfach 100131, 33501 Bielefeld, Germany

Received August 10, 1999

The electronic structure of metallacycloposphazene complexes with several substituents at the phosphorus atoms and metallacyclothiazene complexes is explored for a variety of transition metal elements using density functional theory methods. Accordingly the metallacycloposphazenes possess a large HOMO–LUMO energy separation while the metallacyclothiazenes bear stronger open-shell character. In addition our calculations predict the existence of experimentally so far unknown dimetallacycloposphazenes. All structures show to be highly dynamical. The double bond character of the transition metal nitrogen bond is much less pronounced than in nitrido or imido complexes. For the ring compounds vibrational spectra are reported and compared with experimental data.

## 1. Introduction

Cyclophosphazenes were discovered more than one century ago. In the reaction of phosphorus(V) chloride with ammonium chloride



a cyclotrimer and a cyclotetramer are formed as main products. Because of their structural similarity with the benzene molecule, the cyclotrimers gave rise to some theoretical interest: The cyclotrimer adopts  $D_{3h}$  symmetry, all NP bonds are of equal length ( $\approx 1.6 \text{ \AA}$ ), and intraannular angles of approximately  $120^\circ$  were found<sup>1</sup> (see Figure 1).

Therefore a benzene-like (“aromatic”) delocalization of the  $\pi$  electrons has been assumed. The degree of delocalization has been the subject of a historical controversy:

(i) The model of Craig<sup>2,3</sup> postulates a complete cyclic delocalization of six  $\pi$  electrons. A topological analysis of the molecular orbitals in the basis of the  $p_z$  orbitals of the nitrogen atoms and the d orbitals of the phosphorus atoms demonstrates that the cyclotrimer should be aromatic.

(ii) In the “island model” of Dewar<sup>4</sup>  $\pi$ -delocalization is restricted to groups of only three atoms (i.e.  $\text{P}=\text{N}=\text{P} \leftrightarrow \text{P}=\text{N}-\text{P}$ ). Thus, the electron sextet should remain essentially nondelocalized.

If one makes use of modern quantum chemical methods, the admixture of d orbitals to the  $\pi$  systems is found to be negligible. According to ab initio calculations the phosphorus–nitrogen bond should be described as a strongly polar  $\sigma$  bond.<sup>5,6</sup> A significant charge concentration at the nitrogen atoms can be observed in a population analysis (e.g. utilizing the NBO partitioning scheme;<sup>7</sup> see Table 1); the  $\pi$  electrons have to be

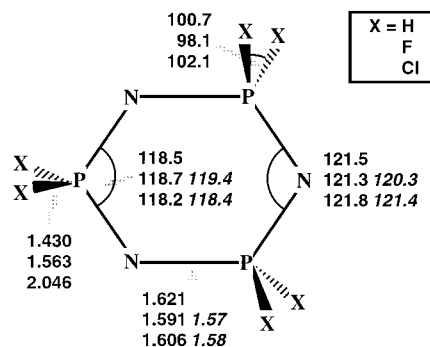


**Figure 1.** Molecular structure of cyclotriphosphazenes with different substituents X = H, F, and Cl at the phosphorus atoms (bond lengths in Å, angles in deg). Our calculated results (at the B3LYP/SBK(d) level) are compared with experimental data<sup>1</sup> (in italics).

**Table 1.** Partial Charges ( $q$ ) and Wiberg Bond Indices ( $b$ ) for Cyclotriphosphazenes, with NBO Analysis at the B3LYP/SBK(d) Level

	$q(\text{N})$	$q(\text{P})$	$q(\text{X})$	$b(\text{PN})$
$\text{N}_3(\text{PH}_2)_3$	-1.49	1.65	-0.08	1.01
$\text{N}_3(\text{PF}_2)_3$	-1.52	2.66	-0.57	1.03
$\text{N}_3(\text{PCl}_2)_3$	-1.47	1.92	-0.23	1.01

characterized as isolated nitrogen lone pairs. Therefore, the Lewis structure given in Chart 1 is a good description for the electronic structure of the cyclotriphosphazenes.

In 1986 the first metallacycloposphazene could be characterized by X-ray diffraction.<sup>8</sup> Formally, this molecule can be constructed by replacing a  $\text{PX}_2^+$  group by a  $\text{WCl}_3^+$  fragment. Later, the synthesis of an analogous derivative of molybdenum succeeded<sup>9</sup> too. In these molecules, the transition metal atom is coordinated by two nitrogen atoms, which are also part of the ring system. A similar connectivity has been found in the cyclic nitrido complexes of these transition metals.<sup>10–13</sup> In this

(1) Krishnamurthy, S. S.; Sau, A. C.; Woods, W. *Adv. Inorg. Radiochem.* **1978**, *21*, 41–112.

(2) Craig, D. P.; Paddock, N. L.; *Nature* **1958**, *181*, 1052–1053.

(3) Craig, D. P.; Mitchell, K. A. R. *J. Chem. Soc.* **1965**, 4682–4690.

(4) Dewar, M. J. S.; Lucken, E. A. C.; Whitehead, M. A. C. *J. Chem. Soc.* **1960**, 2423–2429.

(5) Ahlrichs, R.; Schiffer, H. *J. Am. Chem. Soc.* **1985**, *107*, 6494–6498.

(6) Trinquier, G. *J. Am. Chem. Soc.* **1986**, *108*, 568–577.

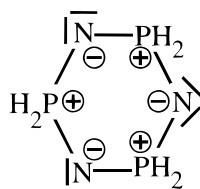
(7) Reed, A. E.; Curtiss, L. A.; Weinhold, F. *Chem. Rev.* **1988**, *88*, 899–926.

(8) Roesky, H. W.; Katti, K. V.; Seseke, U.; Witt, M.; Egert, E.; Herbst, R.; Sheldrick, G. M. *Angew. Chem.* **1986**, *98*, 447–449; *Angew. Chem., Int. Ed. Engl.* **1986**, *25*, 477–479.

(9) Roesky, H. W.; Katti, K. V.; Seseke, U.; Schmidt, H.-G.; Egert, E.; Herbst, R.; Sheldrick, G. M.; *J. Chem. Soc., Dalton Trans.* **1987**, 847–849.

(10) Strähle, J. Z. *Anorg. Allg. Chem.* **1970**, *375*, 238–254.

Chart 1



case, a strong asymmetry in the M–N bonds is observed. Each transition metal center forms one very strong M–N bond of almost triple bond character; the other M–N bond is only a weak donor–acceptor interaction between the nitrogen and the transition metal atom.<sup>14</sup>



Due to these findings, two major questions arise: (i) Is there a considerable amount of  $\pi$  interaction in the transition metal nitrogen bonds? (ii) Are both M–N bonds in the metallacyclophosphazenes of equal strength (i.e. the phosphazene fragment dominates the structure) or are they asymmetrical as in the nitrido complexes?

In the experimental structure, only a weak deformation is observed: Mo–N<sub>1</sub> = 1.766 Å, Mo–N<sub>2</sub> = 1.789 Å;<sup>9</sup> W–N<sub>1</sub> = 1.773 Å, W–N<sub>2</sub> = 1.798 Å.<sup>8</sup> Upon crystallization, an additional solvent molecule (acetonitrile) coordinates to the transition metal atoms. So it is impossible to trace the nature of this asymmetry from experimental evidence alone. Therefore, we carried out DFT calculations for a series of metallacyclophosphazenes, some of which are hitherto experimentally unknown.

## 2. Monometallacyclophosphazenes

### 2.1. Qualitative Considerations for the Electronic Structure.

In a simplified manner, metallacyclophosphazenes can be described by a  $C_{2v}$  symmetrical model structure. In this idealized structure the transition metal atom has a trigonal-bipyramidal ligand field. Two of the chloro ligands occupy the axial positions of the bipyramid. The third chloro ligand and the two coordinating nitrogen atoms are found in the equatorial positions. Similar to the parent cyclophosphazenes, the resulting ring is planar. The actual equilibrium structures of these molecules may be explained as slight distortions from this idealized  $C_{2v}$  structure.

For a qualitative description of the bonding situation, the complex can be formally separated into a  $\text{MCl}_3^{3+}$  fragment and a (chelating)  $[\text{N}_3(\text{PR}_2)_2]^{3-}$  ligand. The corresponding decomposition of molecular orbitals into fragment orbitals is shown in Figure 2.

In the trigonal-planar ligand field of the three chloro ligands the metal d orbitals (Figure 2, left) split up into fragment orbitals of  $a_1$  ( $d_z^2$  and  $d_{x^2-y^2}$ ),  $b_1$  ( $d_{xz}$ ),  $a_2$  ( $d_{xy}$ ), and  $b_2$  symmetry ( $d_{yz}$ ). The relevant fragment orbitals of the phosphazene ligand (Figure 2, right) are formed by a positive ( $a_1$  symmetry) and a negative ( $b_1$  symmetry) linear combination of nitrogen  $sp^2$  hybrids and a positive ( $b_2$  symmetry) and a negative ( $a_2$  symmetry) linear combination of nitrogen  $p_y$  orbitals. Figure 2 shows that the  $a_1$  and the  $b_1$  sets are responsible for the metal–nitrogen  $\sigma$  bonds;

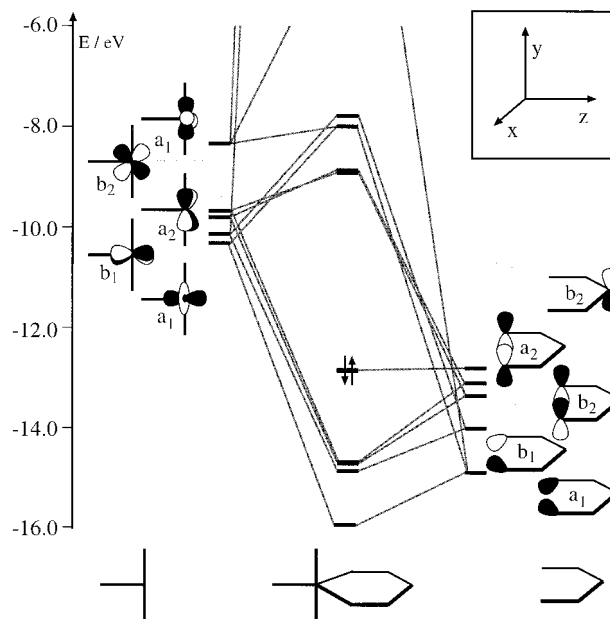


**Figure 2.** Mutual interaction of a  $\text{MoCl}_3^{3+}$  fragment (left) with a  $[\text{N}_3(\text{PH}_2)_2]^{3-}$  ligand (right). All orbitals are classified according to point group  $C_{2v}$ . The orbital energies result from EHT calculations. For clarity, orbitals of minor importance for the Mo–N interaction are omitted. The only exception is the nonbonding HOMO, which is plotted to demonstrate the size of the HOMO–LUMO gap.

the  $b_2$  and  $a_2$  orbital sets form metal–nitrogen  $\pi$  bonds. So the transition metal center acts as a  $\sigma$  and a  $\pi$  acceptor toward our hypothetical phosphazene ligand. This is in contrast to the situation if M is replaced by a  $\text{PX}_2$  group, because the latter is only a  $\sigma$  acceptor. We can demonstrate this difference by a population analysis using the NBO partitioning scheme (see Table 2).

The M–N bond order is always larger than the N–P bond order. As a consequence, the charge separation between the transition metal atom and the nitrogen atom is reduced in comparison with the charge separation between nitrogen and phosphorus (i.e. the partial charge of  $\text{N}_M$  is about 0.5 smaller than that of  $\text{N}_P$ ).

Figure 2 shows, furthermore, that transition metals of group 6 of the periodic table will form closed-shell molecules with a rather large HOMO–LUMO gap. For elements of groups 7 and 8 in their formal oxidation state +VI, for which metallacyclophosphazenes could not be synthesized so far, doublet or triplet ground states have to be expected, respectively. The unpaired electrons in these molecules are predominantly localized in the d shell of the transition metal atom.

### 2.2. Calculated Structural Parameters.

The optimized structures of the metallaphosphazenes are depicted in Figures 3 and 4. Two qualitatively different structures are found depending on the residues “X” at the phosphorus atoms. In case of X = H the molecules adopt  $C_s$  symmetry with the mirror plane oriented perpendicular to the ring plane. In other words, both transition metal nitrogen bonds are equivalent. The phosphazene ring has a chair conformation. For different transition metal atoms the deviations from a planar structure (out of plane angle as defined in Figure 5) range from 15.2° (M = Cr) to 33.0° (M = Os).

If “X” is a halide atom (F or Cl in this study), the rings become planar. For these molecules two M–N bonds of different length are observed. The ring system shows alternating bond lengths, so overall  $C_s$  symmetry results. One exception is the compound with M = Cr, which only has  $C_1$  symmetry. In

- (11) Close, M. R.; McCarley, R. E. *Inorg. Chem.* **1994**, *33*, 4198–4201.
- (12) Chisholm, M. H.; Foltling-Streib, K.; Tiedtke, D. B.; Limoigno, F.; Eisenstein, O. *Angew. Chem.* **1995**, *107*, 61–63; *Angew. Chem., Int. Ed. Engl.* **1995**, *34*, 110–112.
- (13) Herrmann, W. A.; Bogdanovic, S.; Priemermeier, T.; Poli, R.; Fettingner, J. C. *Angew. Chem.* **1995**, *107*, 63–66; *Angew. Chem., Int. Ed. Engl.* **1995**, *34*, 112–115.
- (14) Schoeller, W. W.; Sundermann, A. *Inorg. Chem.* **1998**, *37*, 3034–3039.

**Table 2.** Partial Charges ( $q$ ) and Wiberg Bond Indices ( $b$ ) for Metallacyclotriphosphazenes ( $MCl_3N_3(PX_2)_2$ ), with NBO Analysis at the B3LYP/SBK(d) Level<sup>a</sup>

M	X	$q(M)$	$q(N_M)$	$q(N_P)$	$q(PX_2)$	$b(MN_M)$	$b(PN_M)$	$b(PN_P)$
Cr	H	0.48	-0.67	-1.41	1.54	1.69	0.87	1.04
	F	0.43	-0.81, -0.77	-1.47	1.55	1.46, 1.61	0.94, 0.90	1.01, 1.07
	Cl	0.44	-0.76, -0.72	-1.43	1.53	1.51, 1.62	0.92, 0.88	0.99, 1.03
Mo	H	1.10	-0.90	-1.43	1.54	1.60	0.89	1.03
	F	1.05	-1.04, -0.99	-1.48	1.54	1.35, 1.50	0.99, 0.93	1.00, 1.06
	Cl	1.06	-1.00, -0.94	-1.43	1.50	1.36, 1.53	0.98, 0.91	0.97, 1.04
W	H	1.23	-0.96	-1.44	1.59	1.59	1.03	1.03
	F	1.19	-1.09, -1.04	-1.49	1.54	1.34, 1.49	0.99, 0.94	1.00, 1.06
	Cl	1.21	-1.05, -1.00	-1.44	1.50	1.36, 1.52	0.98, 0.92	0.98, 1.04
Tc	H	0.93	-0.79	-1.43	1.52	1.44	0.89	1.03
Re	H	1.10	-0.86	-1.44	1.53	1.46	0.90	1.03
Ru	H	0.89	-0.74	-1.41	1.51	1.13	0.91	1.03
Os	H	1.08	-0.84	-1.42	1.51	1.21	0.90	1.03

<sup>a</sup>  $N_M$ : nitrogen atom attached to the transition metal atom.  $N_P$ : nitrogen atom bound to two phosphorus atoms. If atoms are not equivalent by symmetry, different charges/bond indices are given, if they differ by more than 0.01. In each case, the nitrogen atom with the larger partial charge, which is always the one with a weaker M–N bond, is given first.

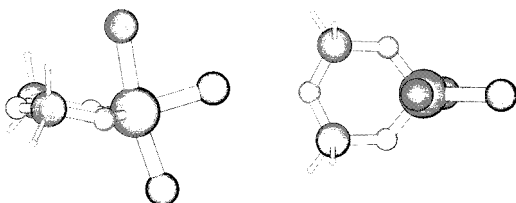


**Figure 3.** Molecular structure of the metallacyclophosphazene  $MoCl_3[N_3(PH_2)_2]$  optimized at the B3LYP/SBK(d) level. Left: Perspective representation of the conformation of the ring. Right: View parallel to the mirror plane demonstrating  $C_s$  symmetry. The mirror plane contains all chlorine atoms and is oriented perpendicular to the ring.

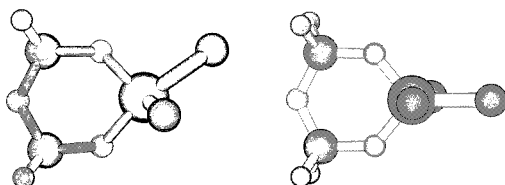


**Figure 4.** Molecular structure of a metallacyclophosphazene with electronegative substituents at the phosphorus atoms.  $MoCl_3[N_3(PF_2)_2]$  and  $MoCl_3[N_3(PCl_2)_2]$  adopt the same structure. Left: Equilibrium structure of  $C_s$  symmetry; the ring is planar. Right: Transition state for the degenerate rearrangement ( $C_{2v}$  symmetry). Both structures are optimized at the B3LYP/SBK(d) level.

	N	M	
	22.8	15.2	Cr
	25.8	19.9	Mo
	22.5	16.3	W
	28.4	25.2	Tc
	27.4	24.2	Re
	29.6	31.5	Ru
	29.1	33.0	Os

**Figure 5.** Deviations from a planar ring structure (out of plane angles in deg) in the metallacyclophosphazenes  $MCl_3[N_3(PH_2)_2]$ . Other structural parameters are given in Figure 6.

this case, also a slight distortion of the ring towards a chair conformation is found, in addition to alternating bond lengths. Our calculated structural parameters are listed in the Figures 6–8. For comparison, experimental results are given in Figure 9.

Our calculations show a quite good agreement with the experimental structures. Interestingly, the alternation of bond

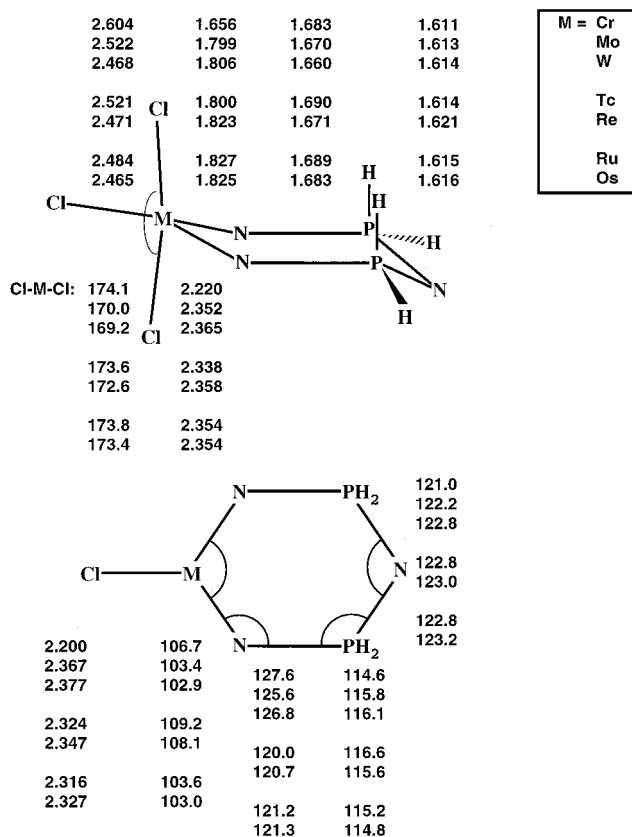


**Figure 6.** Optimized structural parameters for metallacyclophosphazenes  $MCl_3[N_3(PH_2)_2]$  (distances in Å, angles in deg). All molecules adopt  $C_s$  symmetry. The corresponding electronic states are the following: Cr, Mo, W,  $^1A'$ ; Tc, Re,  $^2A'$ ; Ru, Os,  $^3A''$ .

lengths in the ring is reproduced by the calculations on the chlorine and fluorine derivatives. So the distorted structure is intrinsic to the metallacyclophosphazene system. Optimizations of the corresponding  $C_{2v}$  structure, which turns out to be the transition state for a degenerate rearrangement  $C_s \rightarrow C_{2v} \rightarrow C'_s$ , reveals a very low barrier (see Table 3). Therefore, rapid rearrangements have to be expected at room temperature. It would be interesting to test this prediction by NMR spectroscopy.

In comparison with the corresponding parent cyclophosphazenes the length of the P– $N_P$  bond is not altered very much if one  $PX_2$  group is replaced by a transition metal complex fragment. The P– $N_M$  bond on the other hand, is always longer

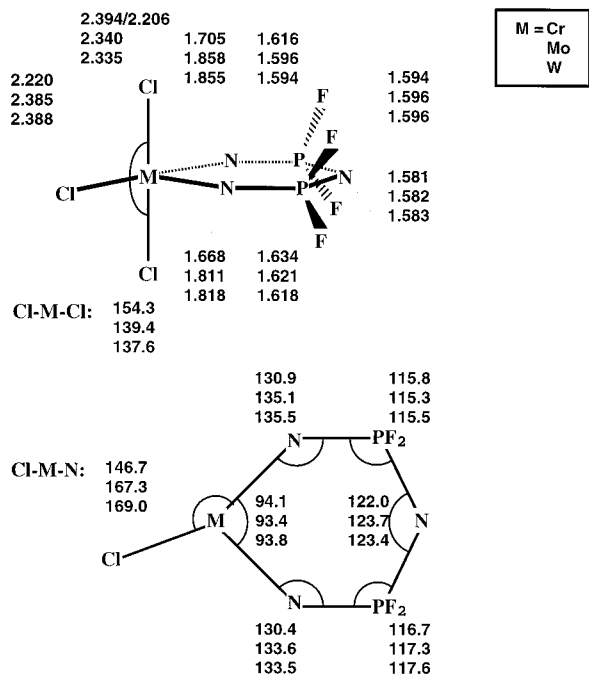


**Figure 7.** Optimized structural parameters for metallaphosphazenes  $MCl_3[N_3(PF_2)_2]$  (distances in Å, angles in deg). All molecules except the case  $M = Cr$  adopt  $C_s$  symmetry; the mirror plane contains the ring.

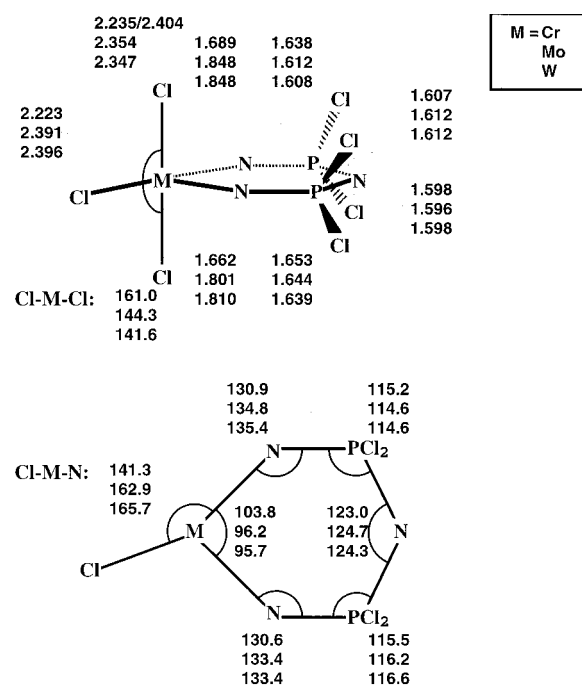


**Figure 8.** Optimized structural parameters for metallaphosphazenes  $MCl_3[N_3(PCl_2)_2]$  (distances in Å, angles in deg). These compounds are isostructural to the corresponding fluoro derivatives.

in the metalla derivatives. The  $M-N$  bond weakens the  $N-P$  bond. This can be explained by the description of the  $N-P$  bond as a polar  $\sigma$  bond: Because the bond strength is enhanced by the polarity of the bond, a reduction of the charge density at the nitrogen atom will result in a weaker bond. As we demonstrated by the results of the population analysis given in Table 2, the transition metal atom is a  $\pi$  acceptor. Therefore, charge density is transferred from  $N_M$  to  $M$  and this causes the increase of the  $P-N_M$  distance.

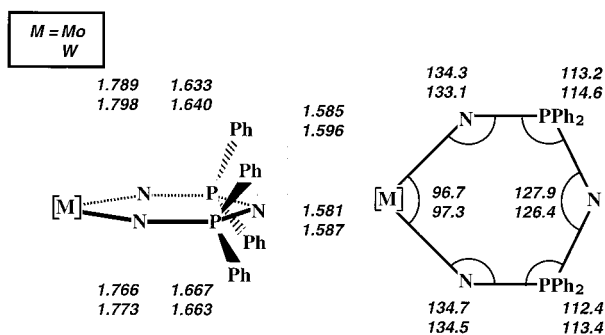


**Figure 9.** Experimental structural parameters<sup>8,9</sup> for metallaphosphazenes  $MCl_3[N_3(PPh_2)_2]$  (distances in Å, angles in deg). In the crystal structure an additional acetonitrile ligand binds toward the transition metal atom.

### Chart 2

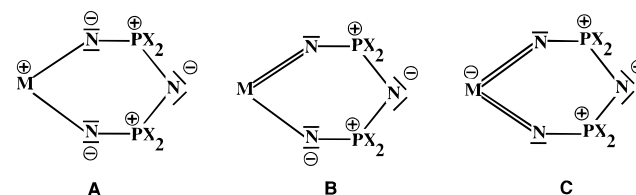


**Table 3.** Energies (in  $\text{kJ}\cdot\text{mol}^{-1}$ ) of the  $C_{2v}$  Transition State Relative to the Ground State ( $C_s$ ) of Metallacycloposphazenes Calculated at the B3LYP/SBK(d) Level

M	X	$\Delta E$ ( $\text{kJ}\cdot\text{mol}^{-1}$ )	M	X	$\Delta E$ ( $\text{kJ}\cdot\text{mol}^{-1}$ )
Mo	H	5.9	W	H	1.2
	Cl	2.6		Cl	4.6
	F	7.6		F	8.5

The results of the population analyses are depicted in Chart 2. Lewis structure **A** corresponds to the classical cyclophosphazene ( $M = PX_2$ ). It is identical with the one given in Chart 1. Because of the  $\pi$  acceptor ability of the transition metal atoms; Lewis structure **B** or **C** will give a better description of the electronic structure of metallacycloposphazenes. In **B** one transition metal nitrogen double bond is formed. In **C** the  $\pi$  donation is even stronger; therefore, one negative charge is formally localized on the transition metal atom and the transition metal nitrogen bonds are equivalent. It depends on the donor strength of the phosphazene ligand whether **B** or **C** is favored. According to our calculations, Lewis structure **B** is realized if  $X$  is an electronegative substituent, which reduces the negative charge at the nitrogen atoms. Structures with different  $M-N$  bond lengths are found for  $X = F$  and  $Cl$ . In the case of  $X = H$  the electronic structure is best described by **C**. This becomes apparent in the NBO analysis, which clearly assigns double bond character to both  $M-N$  bonds.

A comparison of different metallacycloposphazenes shows that the molecular structure is, at least on a qualitative level, independent of the choice of the transition metal atom. Within a given group of transition metals the  $M-N$  distances increase from the top to the bottom (e.g.  $Cr < Mo < W$ ), and within a given period they increase from the left to the right (i.e.  $Mo < Tc < Ru$ ,  $W < Re < Os$ ). This trend within a period may be explained on the basis of the MO scheme in Figure 2: If  $M$  is an element of group 6 ( $Mo$ ,  $W$ ), the  $d$  shell is empty. For elements of the group 7 one and for those of group 8 two more  $d$  electrons are involved. Because the corresponding  $d$  orbitals are  $M-N$  antibonding, the  $M-N$  bond becomes weaker. This can also be demonstrated by a calculation of the stabilization energies (see Table 4), according to eq 3:  $MNCl_3$  is the

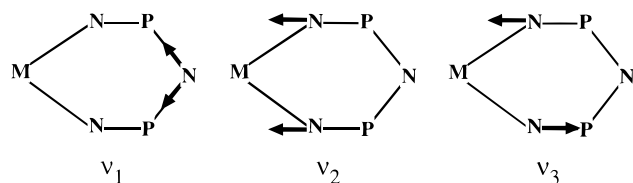
**Table 4.** Stabilization Energies According to Eq 3 Calculated at the B3LYP/SBK(d) Level

M	$\Delta E$ (kJ·mol <sup>-1</sup> )
Cr	-143.2
Mo	-227.7
W	-297.1
Tc	-158.4
Re	-217.3
Ru	-139.2
Os	-180.2

**Table 5.** Vibrational Frequencies for the N–P Stretching Modes in Metallacycloposphazenes (in cm<sup>-1</sup>) Calculated at the B3LYP/SBK(d) Level within the Harmonic Approximation<sup>a</sup>

M	X	$\nu_{N-P}$ (cm <sup>-1</sup> )	
		calcd	expt
	H	1217 (e'), 1214 (a'2)	
	F	1290 (e'), 1192 (a'2)	1300 <sup>1</sup>
	Cl	1203 (e'), 1119 (a'2)	1218 <sup>1</sup>
Cr	H	1215 (a''), 1087 (a'), 1061 (a'')	
	F	1269 (a'), 1125 (a'), 986 (a')	
	Cl	1191 (a'), 1080 (a'), 938 (a')	
Mo	H	1211 (a''), 1081 (a'), 1049 (a'')	1250, 1175 (for X = Ph) <sup>9</sup>
	F	1272 (a'), 1162 (a'), 1012 (a')	
	Cl	1193 (a'), 1109 (a'), 949 (a')	
W	H	1215 (a''), 1119 (a'), 1077 (a'')	
	F	1272 (a'), 1196 (a'), 1041 (a')	
	Cl	1193 (a'), 1146 (a'), 984 (a')	
Re	H	1208 (a''), 1055 (a'), 1025 (a'')	
Ru	H	1202 (a'), 1019 (a'), 963 (a'')	
Os	H	1203 (a''), 1001 (a'), 998 (a'')	

<sup>a</sup> The corresponding normal modes are depicted in Chart 3.

**Chart 3**

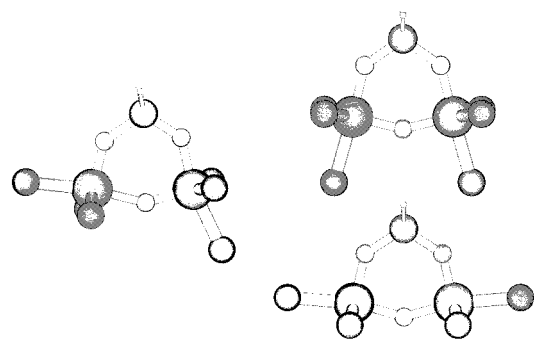
corresponding nitrido complex;<sup>15</sup> (NPH<sub>2</sub>)<sub>2</sub> is a cyclodiphosphazene.<sup>5,6</sup> For all transition metals this reaction was found to



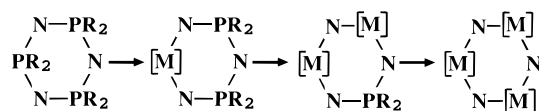
be strongly exothermic ( $300 \geq \Delta E \geq 140$  kJ·mol<sup>-1</sup>). The largest stabilization energy is calculated for M = W. It decreases in a group of transition metals from bottom to top and within a period from left to right. This finding is in line with the trend we found for the M–N distances.

**2.3. Vibrational Spectra.** The vibrational frequencies of the N–P stretching modes calculated within the harmonic approximation are given in Table 5. For all metallacycloposphazenes there is one band ( $\nu_1$ ) that matches the transition in the cyclophosphazenes; two other modes ( $\nu_2$  and  $\nu_3$ ) are found at smaller wavenumbers. A depiction of the corresponding normal modes is given in Chart 3.

The normal mode  $\nu_1$  is mainly restricted to displacements of N<sub>P</sub> from its equilibrium position. Therefore its frequency is not shifted very much relative to the value found for the cyclophosphazenes. The modes  $\nu_2$  and  $\nu_3$  are a positive and a negative linear combination of the P–N<sub>M</sub> stretches. In the



**Figure 10.** Equilibrium structures of dimetallacycloposphazenes. (As an example, the complex (MoCl<sub>3</sub>)<sub>2</sub>N<sub>3</sub>(PH<sub>2</sub>) is shown.) All three structures are local minima for M = Mo, W and X = H, F, Cl. The left structure is C<sub>s</sub> symmetric; the two on the right have C<sub>2v</sub> symmetry. The lower right structure (“C<sub>2v</sub>-a”) is the energetically most favorable conformation. The C<sub>s</sub> conformer is found to be only a few kJ·mol<sup>-1</sup> higher in energy. The third local minimum (“C<sub>2v</sub>-b”) is about 20 kJ·mol<sup>-1</sup> less stable.

**Scheme 1**

halide-substituted compounds these modes have the same symmetry (a'). Thus, the coupling of these modes is rather strong and a splitting of 150 cm<sup>-1</sup> is found. If X is a hydrogen atom, the modes have different symmetries and the splitting reduces to 20–40 cm<sup>-1</sup>.

### 3. Dimetallacycloposphazenes

We will now extend our computational study to an experimentally so far unknown class of compounds: the dimetallacycloposphazenes. These complexes are of theoretical interest, because they can be regarded as a missing link between the cyclophosphazenes and the oligomers of nitrido complexes (Scheme 1).

In the dimetallacycloposphazenes a nitrogen atom forms a  $\mu_2$  bridge between two transition metal atoms. Again, the question arises whether this bridge is symmetrical or asymmetrical as in the nitrido complexes of transition metals of the group 6 of the periodic table.

**3.1. Optimized Structures.** Surprisingly, our calculations predict three local minima on the potential energy hypersurface for M = Mo and W. Two of them are almost degenerate; the third one is somewhat higher in energy. For M = Cr only one minimum could be found. The molecular structures for all these minima are depicted in Figure 10.

In more detail, the minima can be described as follows:

**One Minimum of C<sub>s</sub> Symmetry.** (For structural parameters see Figure 11.) In this conformation the molecule adopts a planar ring with alternating bond lengths. The difference between the long and short M–N bonds in the dimetalla-substituted ring systems ( $\Delta r = 0.18$  Å (M = Mo), 0.10 Å (M = W)) is much more pronounced than in systems containing only one transition metal atom ( $\Delta r \approx 0.05$  Å). But this bond length alternation is still smaller than it was found in the cyclotrimers of nitrido complexes<sup>14</sup> ( $\Delta r \approx 0.5$  Å (M = Mo), 0.3 Å (M = W)). The different M–N bond lengths also enforce different N–P distances. The N–P–N angle is about 6° smaller than in the cyclophosphazenes. This is comparable to the value found for the monometalla derivatives. Interestingly, the M–N–M angle

(15) Sundermann, A. The Transition-Metal-Nitrogen Bond: Quantum Chemical Calculations on Selected Systems. Ph.D. Dissertation, Universität Bielefeld, 1999.

	H	F	Cl		H	F	Cl		H	F	Cl
Mo	1.698	1.665	1.686	Mo	112.1	112.6	111.2	Mo	1.595	1.553	1.569
W	1.676	1.639	1.658	W	112.5	113.5	112.0	W	1.606	1.560	1.584

	H	F	Cl		H	F	Cl
Mo	139.8	142.1	142.1	Mo	135.4	134.6	135.6
W	137.9	139.0	139.2	W	136.2	135.6	136.6

	H	F	Cl		H	F	Cl
Mo	1.770	1.772	1.769	Mo	1.896	1.943	1.931
W	1.791	1.800	1.796	W	1.872	1.897	1.890

	H	F	Cl		H	F	Cl
Mo	92.8	92.4	92.4	Mo	92.8	92.4	92.4
W	92.4	91.9	91.9	W	92.4	91.9	91.9

	H	F	Cl		H	F	Cl
Mo	89.9	88.1	88.6	Mo	1.761	1.747	1.749
W	91.4	90.1	90.5	W	1.793	1.788	1.789

	H	F	Cl		H	F	Cl
Mo	1.956	1.986	1.979	Mo	150.0	150.2	150.1
W	1.909	1.917	1.915	W	149.6	149.9	149.7

**Figure 11.** Selected bond lengths (in Å) and angles (in deg) in the  $C_s$  conformer of dimetallaphosphazenes.

	H	F	Cl		H	F	Cl		H	F	Cl
Cr	132.6	133.6	133.9	Cr	114.2	114.4	113.2	Cr	1.654	1.617	1.637
Mo	135.8	136.0	136.7	Mo	114.5	115.6	114.0	Mo	1.646	1.609	1.628
W	135.6	135.5	136.2	W	114.7	116.0	114.4	W	1.643	1.607	1.625

	H	F	Cl		H	F	Cl
Cr	94.5	93.0	93.5	Cr	1.681	1.701	1.692
Mo	92.6	91.5	91.8	Mo	1.811	1.818	1.821
W	92.9	92.1	92.3	W	1.815	1.830	1.825

	H	F	Cl		H	F	Cl
Cr	2.257	2.248	2.254	Cr	2.220	2.205	2.210
Mo	2.388	2.381	2.385	Mo	2.334	2.320	2.325
W	2.393	2.385	2.389	W	2.332	2.319	2.323

	H	F	Cl		H	F	Cl
Cr	151.6	152.4	152.0	Cr	1.724	1.728	1.726
Mo	148.8	149.4	149.1	Mo	1.861	1.864	1.862
W	148.5	148.8	148.6	W	1.857	1.859	1.858

**Figure 12.** Selected bond lengths (in Å) and angles (in deg) in the  $C_{2v}$ -a conformer of dimetallaphosphazenes.

( $\approx 150^\circ$ ) is only by  $5^\circ$  smaller than the corresponding angle in the nitrido rings. Both transition metal centers have a distorted tetragonal-pyramidal ligand field; the tighter bound nitrogen atom occupies the apical position.

**One Minimum with  $C_{2v}$  Symmetry (" $C_{2v}$ -a").** (Structural parameters are given in Figure 12.) In this conformer a symmetrical nitrido bridge between the two transition metal centers is formed. The  $M-N_M$  distances of 1.86 Å and the  $M-N_P$  of 1.82 Å are close to the averages of the long/short distances in the  $C_s$  structure. Both transition metal atoms are again coordinated tetragonal-pyramidally. The shorter  $M-N$  distance occurs for the nitrogen atom occupying the apical position of the pyramid. In this conformer, the phosphorus atom forms two equivalent  $N-P$  bonds. They are elongated by 0.1–0.2 Å in comparison with the corresponding cyclotriphosphazenes. For the case  $M = Cr$  this conformer is found to be the only minimum.

**Second Minimum with  $C_{2v}$  Symmetry (" $C_{2v}$ -b").** (For structural parameters, see Figure 13.) This conformer differs from the previous one in the arrangement of the chloro ligands. Here, a trigonal-bipyramidal ligand field is found. The metal phosphorus bridging nitrogen atom  $N_P$  occupies an axial position of this bipyramid in *trans* position of a chloro ligand. This

	H	F	Cl		H	F	Cl
Mo	110.3	110.9	109.6	Mo	138.4	138.9	139.4
W	110.5	111.5	110.2	W	138.4	138.5	139.1

	H	F	Cl		H	F	Cl
Mo	1.638	1.600	1.616	Mo	1.853	1.876	1.869
W	1.634	1.598	1.613	W	1.846	1.864	1.859

	H	F	Cl		H	F	Cl
Mo	90.1	88.7	89.1	Mo	2.398	2.387	2.391
W	90.9	89.8	90.0	W	2.401	2.390	2.393

	H	F	Cl		H	F	Cl
Mo	152.6	153.8	153.3	Mo	1.831	1.830	1.830
W	150.9	151.9	151.6	W	1.836	1.836	1.836

**Figure 13.** Selected bond lengths (in Å) and angles (in deg) in the  $C_{2v}$ -b conformer of dimetallaphosphazenes.

**Table 6.** Energies (in  $\text{kJ}\cdot\text{mol}^{-1}$ ) of the  $C_s$  and the  $C_{2v}$ -b Conformer Relative to the Ground State ( $C_{2v}$ -a) Calculated at the B3LYP/SBK(d) Level

M	X	$\Delta E(C_s)$	$\Delta E(C_{2v}\text{-b})$
Mo	H	9.4	27.6
	Cl	2.1	16.9
	F	2.5	18.4
W	H	13.0	30.7
	Cl	7.2	20.1
	F	8.0	21.6

causes a weakening of both the  $M-N_P$  and the  $M-Cl_{ax}$  bonds, as is witnessed in an increase of the corresponding distances relative to conformer  $C_{2v}$ -a. The  $M-N_M$  and the  $N_P-P$  bonds on the other hand become shorter.

As a summary, we can state that there are conformers with a cyclophosphazene-like structure ( $C_{2v}$ ) and another one which is dominated by structure elements from nitrido complexes ( $C_s$ ). The relative energies of these local minima are given in Table 6.

All energy differences are found to be rather small. From the results obtained for the monometalla derivatives one may deduce that the transition states for rearrangements from one conformer to another are also low in energy. So the energy hypersurface is very flat and the dimetallacyclophosphazenes are expected to have fluctuating structures.

**3.2. Qualitative Considerations.** In Tables 7 and 8 results of a population analysis for the dimetallacyclophosphazenes are given.

There are no significant differences between the partial charges of the transition metal atoms, the  $PX_2$  groups, and the nitrogen atoms  $N_P$  found for these complexes and those calculated for the monometalla derivatives. The concentration of negative charge on  $N_M$  is rather small. A partial charge of  $\approx -0.5$  is comparable to the value found for nitrido complexes.<sup>14</sup>

An analysis of the bond indices reveals that in the  $C_{2v}$  symmetrical conformers all  $M-N$  bonds have some double bond character. For the  $C_s$  structure, an alternation in bond orders is observed.

The electronic structure of the dimetallacyclophosphazenes can be expressed by the Lewis structures shown in Chart 4. In the  $C_s$  symmetrical structure one Lewis structure dominates, e.g.:

$$\Psi_{C_s} \approx \Psi_A \quad (4)$$

For the  $C_{2v}$  symmetrical conformers, on the other hand, both Lewis structures are of equal importance. They have to be interpreted as resonance structures. The double bonds are

**Table 7.** Partial Charges ( $q$ ) and Wiberg Bond Indices ( $b$ ) for Dimetallacycloposphazenes with  $C_{2v}$  Structure: Results of a NBO Analysis of the Charge Density at the B3LYP/SBK(d) Level<sup>a</sup>

M	X	$q(M)$	$q(N_M)$	$q(N_P)$	$q(PX_2)$	$b(MN_M)$	$b(MN_P)$	$b(PN_P)$
$C_{2v}$ -a Symmetry								
Cr	H	0.33	-0.15	-0.71	1.49	1.27	1.54	0.95
	F	0.32	-0.14	-0.80	1.51	1.26	1.43	0.97
	Cl	0.33	-0.14	-0.76	1.50	1.27	1.46	0.95
Mo	H	1.01	-0.51	-0.92	1.54	1.29	1.50	0.95
	F	1.00	-0.50	-0.99	1.53	1.28	1.41	0.97
	Cl	1.01	-0.50	-0.95	1.50	1.28	1.43	0.96
W	H	1.16	-0.61	-0.97	1.56	1.29	1.51	0.95
	F	1.15	-0.61	-1.05	1.54	1.28	1.41	0.97
	Cl	1.16	-0.61	-1.01	1.52	1.28	1.43	0.98
$C_{2v}$ -b Symmetry								
Mo	H	1.00	-0.51	-0.92	1.54	1.37	1.40	0.96
	F	1.00	-0.50	-0.99	1.53	1.38	1.30	0.99
	Cl	1.00	-0.50	-0.96	1.48	1.38	1.30	0.98
W	H	1.16	-0.62	-0.98	1.55	1.36	1.41	0.96
	F	1.15	-0.61	-1.05	1.53	1.36	1.31	0.99
	Cl	1.15	-0.61	-1.01	1.49	1.36	1.32	0.97

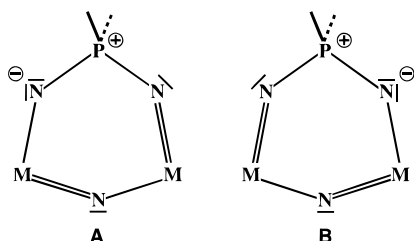
<sup>a</sup>  $N_M$ : nitrogen atom bridging the transition metal centers.  $N_P$ : nitrogen atom connected with the phosphorus atom.

**Table 8.** Partial Charges ( $q$ ) and Wiberg Bond Indices ( $b$ ) for Dimetallacycloposphazenes with  $C_s$  Structure: Results of a NBO Analysis of the Charge Density at the B3LYP/SBK(d) Level<sup>a</sup>

M	X	$q(N_1)$	$q(N_2)$	$q(N_3)$	$b(M_1N)$	$b(M_2N)$	$b(PN)$
Mo	H	-0.51	-1.01	-0.81	1.72, 1.20	0.95, 1.71	0.82, 1.11
	F	-0.50	-1.11	-0.85	1.81, 1.01	0.86, 1.68	0.81, 1.20
	Cl	-0.49	-1.06	-0.83	1.79, 1.04	0.88, 1.69	0.80, 1.16
W	H	-0.61	-1.04	-0.91	1.57, 1.28	1.64, 1.08	0.86, 1.05
	F	-0.61	-1.12	-0.97	1.60, 1.15	1.57, 1.05	0.87, 1.10
	Cl	-0.61	-1.07	-0.94	1.60, 1.17	1.60, 1.06	0.86, 1.08

<sup>a</sup> The partial charges of the transition metal atoms and the  $PX_2$  group are not listed, because they do not differ from the  $C_{2v}$  isomers.  $N_1$ : nitrogen atom bridging the transition metal centers.  $N_2$ : nitrogen atom with a short M–N bond.  $N_3$ : nitrogen atom with a short N–P bond.

#### Chart 4



delocalized over some part of the ring system, according to

$$\Psi_{C_{2v}} \approx \frac{1}{\sqrt{2}}(\Psi_A + \Psi_B) \quad (5)$$

Therefore, the size of the energy difference between  $C_s$  and  $C_{2v}$ -a structure can be explained as follows: In the  $C_{2v}$  structure the coordination of the phosphorus atom is optimal (i.e. comparable to the parent cyclophosphazene), whereas in the  $C_s$  structure an optimal coordination of the transition metal atoms is found. In the latter case, coordination of the transition metal atoms is similar to the nitrido complexes. The phosphorus atom is less favorably coordinated in this case: One N–P bond is stretched; the other one is shortened. Because the phosphorus atom does not act as a  $\pi$  acceptor toward the nitrogen atom, this shortening has no stabilizing effect on the system. The destabilizing effects in  $C_s$  and  $C_{2v}$ -a are almost of the same magnitude, so both

conformers are almost degenerate. In conformation  $C_{2v}$ -b the arrangement of ligands is much more disadvantageous; one chloro ligand is found in the *trans* position of the strong  $\pi$ -donating nitrogen atom. Due to the *trans* influence, this chloro ligand is weaker bound, as is witnessed in the larger M–Cl distance. Therefore, this structure is considerably higher in energy.

**3.3. Conclusion.** The energy differences between the conformations we found for the dimetallacycloposphazenes are rather small. This should cause on one hand a fluctuating structure with interesting dynamics. On the other hand, the influence of the solvent or other intermolecular interactions in the crystal may change the energetic order of the conformers. Only the experiment can decide which conformer is the most stable in condensed matter. A dimetallacycloposphazene is the missing link in the sequence  $N_3(PR_2)_3 \rightarrow MCl_3(N_3(PR_2)_2) \rightarrow (MCl_3)_2(N_3(PR_2)) \rightarrow (MCl_3)_3(N_3)$ . Therefore, its preparation should be an interesting challenge within experimental inorganic chemistry.

#### 4. Metallacyclothiazenes

The first metallacyclothiazene ( $[VCl_2(N_3S_2)]_\infty$ ) could be synthesized by Roesky et al. in 1983.<sup>16</sup> This synthesis has been optimized by Dehnicke et al.<sup>17</sup> and transferred to other transition metals (molybdenum<sup>18</sup> and tungsten<sup>19</sup>). These compounds can be derived formally from the  $[S_3N_3]^-$  ion by substitution of a sulfur atom by an isoelectronic transition metal fragment.

**4.1. The  $[S_3N_3]^-$  Anion.** This anion was first characterized by Chivers et al. The single-crystal X-ray diffraction of a tetrabutylammonium salt revealed an almost planar ring structure with average bond lengths of 1.6 Å.<sup>20–24</sup> Approximately,  $D_{3h}$  symmetry was found. Using topological arguments, a benzene-like  $\pi$  system can be constructed (see Figure 14).

The  $\pi$  system of  $[S_3N_3]^-$  consists of 10 electrons. The negative charge of this anion is completely delocalized. In contrast to the six  $\pi$  electron system benzene, not only the binding  $\pi$  orbitals are occupied but also the antibonding  $e''$  set is filled. Because of this occupation of  $\pi^*$  orbitals the stabilizing effect of the  $\pi$  electron delocalization is expected to be small.<sup>24</sup> This can also be demonstrated by the results of our calculations at B3LYP/SBK(d + diff) level. The calculated bond order from a NBO analysis is only 1.08. Additionally, a large charge separation between nitrogen and sulfur atoms is observed ( $q(N) = -1.10$ ,  $q(S) = 0.77$ ). This charge separation gives evidence to the suggestion that the electronic structure of  $[S_3N_3]^-$  is similar to that of cyclophosphazenes.

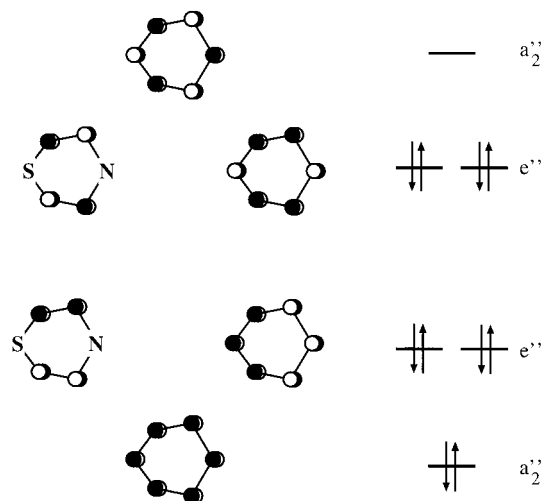
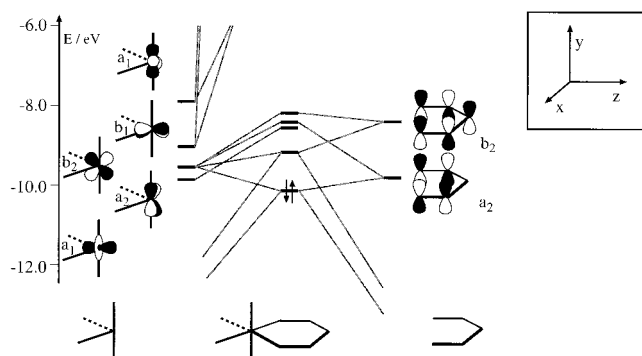
**4.2. Experimental Structures of Metallacyclothiazenes.** The vanadium complex ( $[VCl_2(N_3S_2)]_\infty$ )<sup>16,17</sup> is a polymer. For the salts  $[AsPh_4]^+ [MCl_4(N_3S_2)]^-$ , M = Mo and W crystal structures are available.<sup>18,19</sup> Accordingly, the transition metal atom is coordinated in a distorted octahedral ligand field formed by four

- Roesky, H. W.; Anhaus, J.; Schimdt, H. G.; Sheldrick, G. M.; Noltemeyer, M. *J. Chem. Soc., Dalton Trans.* **1983**, 1207–1209.
- Hanich, J.; Krestel, M.; Müller, U.; Dehnicke, K. *Z. Naturforsch.* **1984**, *39b*, 1686–1695.
- Kynast, U.; Conradi, E.; Müller, U.; Dehnicke, K. *Z. Naturforsch.* **1984**, *39b*, 1680–1685.
- Wadle, H.; Conradi, E.; Müller, U.; Dehnicke, K. *Z. Naturforsch.* **1986**, *41b*, 429–435.
- Bojes, J.; Chivers, T. *Inorg. Chem.* **1978**, *17*, 319–321.
- Bojes, J.; Chivers, T.; Drummond, I.; McLean, G. *Inorg. Chem.* **1978**, *17*, 3668–3672.
- Bojes, J.; Chivers, T. *J. Chem. Soc., Chem. Commun.* **1978**, 391–392.
- Bojes, J.; Chivers, T.; Laidlaw, W. G.; Trsic, M. *J. Am. Chem. Soc.* **1979**, *101*, 4517–4522.
- Gleiter, R. *Angew. Chem.* **1981**, *93*, 442–450; *Angew. Chem., Int. Ed. Engl.* **1981**, *20*, 444–452.

**Table 9.** Partial Charges ( $q$ ) and Wiberg Bond Indices ( $b$ ) for Metallacyclothiazenes (NBO Analysis at the B3LYP/SBK(d + diff) Level)<sup>a</sup>

M	$q(\text{MCl}_4)$	$q(\text{N}_M)$	$q(\text{N}_S)$	$q(\text{S})$	$b(\text{MN})$	$b(\text{N}_M\text{--S})$	$b(\text{N}_S\text{--S})$
Cr	-0.94	-0.65	-1.06	1.15	0.83, 0.86	1.63	1.10
Mo	-0.57	-0.80, -0.77	-0.99	1.04, 1.09	1.28, 1.11	1.26, 1.36	1.15, 1.19
W	-0.48	-0.82	-0.96	1.04	1.26	1.20	1.25

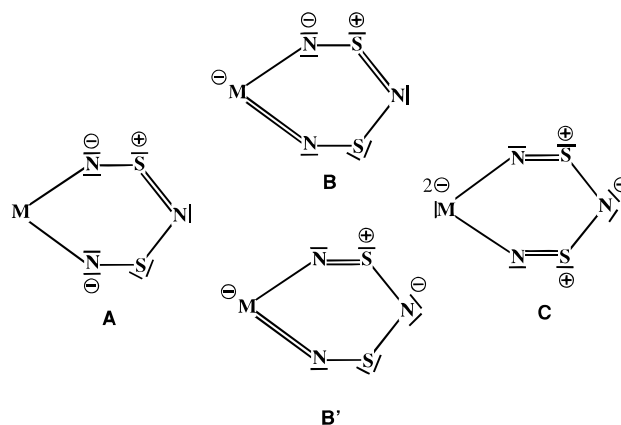
<sup>a</sup>  $\text{N}_M$ : nitrogen atom connected with a transition metal atom.  $\text{N}_S$ : nitrogen atom connected with sulfur atoms only. For nonequivalent atoms, partial charges are given, if they differ by more than 0.01

**Figure 14.** Energy splitting of the  $\pi$  electrons in the  $[\text{S}_3\text{N}_3]^-$  ion. Symmetry classification is according to the point group  $D_{3h}$ .**Figure 15.** Qualitative MO diagram for the interaction of a  $[\text{MoCl}_4]^{2+}$  fragment with a  $[\text{S}_2\text{N}_3]^{3-}$  fragment (from a EHT calculation). Symmetry classification is according to the point group  $C_{2v}$ . Only the frontier orbitals are given.

chloro ligands and two nitrogen atoms of the thiazeno fragment. The anions adopt approximately a  $C_{2v}$  symmetrical structure. In both compounds the M–N bonds are slightly longer than those found for the metallacyclophosphazenes. The N–S distances of 1.54–1.61 Å do not differ very much from  $[\text{S}_3\text{N}_3]^-$ .

**4.3. Electronic Structure of Metallacyclothiazenes.** In Figure 15 a MO diagram for the interaction of a  $[\text{MCl}_4]^{2+}$  fragment with a  $[\text{S}_2\text{N}_3]^{3-}$  fragment is shown. The orbitals have been classified according to  $C_{2v}$  symmetry. The transition metal  $d$  orbitals show a splitting pattern similar to that of the metallacyclophosphazenes (see Figure 2).

Again, the M–N  $\sigma$  bond is formed by orbitals of  $a_1$  and  $b_1$  symmetry;  $\pi$  bonding results from interaction of fragment orbitals of  $a_2$  and  $b_2$  symmetry. EHT calculations show that the HOMO of the metallacyclothiazene is built from a N–S antibonding  $\pi$  orbital and the  $d_{xy}$  orbital of the transition metal atom. The HOMO–LUMO gap turns out to be quite small in the EHT calculation. A DFT calculation reveals a singlet–triplet

**Chart 5**

separation of only 28  $\text{kJ}\cdot\text{mol}^{-1}$  ( $\text{M} = \text{Mo}$ ) favoring the singlet state.

In Table 9 the results of a population analysis are given. Accordingly, the transition metal atom acts as an acceptor toward the thiazeno ligand. Because the corresponding donor orbitals have N–S antibonding character, this charge donation causes a strengthening of the N–S bonds (i.e. in comparison with  $[\text{S}_3\text{N}_3]^-$  the N–S bond order increases). Depending on the  $\pi$  acidity of the transition metal atom, the electronic structure of metallacyclothiazenes may be described by one of the Lewis structures shown in Chart 5.

Lewis structure **A** corresponds to the  $[\text{S}_3\text{N}_3]^-$  ion, if “M” is replaced by a sulfur atom. But our population analyses reveal that a transition metal atom in its formal oxidation state +VI is a better  $\pi$  acceptor than a sulfur atom. Therefore, the complex fragment  $\text{MCl}_4$  is negatively charged and a positive charge of almost 1.0 is delocalized over the group S–N<sub>3</sub>–S. According to the NBO analysis, we can differentiate two groups of complexes: In the compounds of molybdenum and tungsten, the electronic structure is dominated by the Lewis structures **B** and **B'**. In case of  $\text{M} = \text{Mo}$  the localization of double bonds (i.e. Lewis structure **B'**) is more pronounced than for  $\text{M} = \text{W}$ . For the chromium complex, Lewis structure **C** is of major importance. This means an electron pair is completely transferred to the transition metal atom. In the MO picture this can be described by a HOMO, which is localized at the chromium atom (i.e. the transition metal  $d$  orbital is so low in energy that  $[\text{M}]$  has to be assigned as the donor and  $[\text{S}_2\text{N}_3]^-$  as the acceptor). Therefore, this compound should be characterized as a chromium(IV) rather than as a chromium(VI) complex.

**4.4. Calculated Equilibrium Structures.** The optimized equilibrium structures for metallathiazene complexes  $[\text{MCl}_4(\text{N}_3\text{S}_2)]^-$  adopt  $C_s$  symmetry for  $\text{M} = \text{Cr}$  and  $\text{Mo}$  (mirror plane = ring plane) and  $C_{2v}$  symmetry for  $\text{M} = \text{W}$ . The calculations show that the potential energy surface is very flat with respect to a deformation of the ring, according to  $C_{2v} \rightarrow C_s$  (e.g. for  $\text{M} = \text{Mo}$  a transition state of  $C_{2v}$  symmetry is only 0.1  $\text{kJ}\cdot\text{mol}^{-1}$  less stable than the  $C_s$  ground state). So facile distortions of the ring have to be expected. The optimized structure parameters are given in Figure 16.



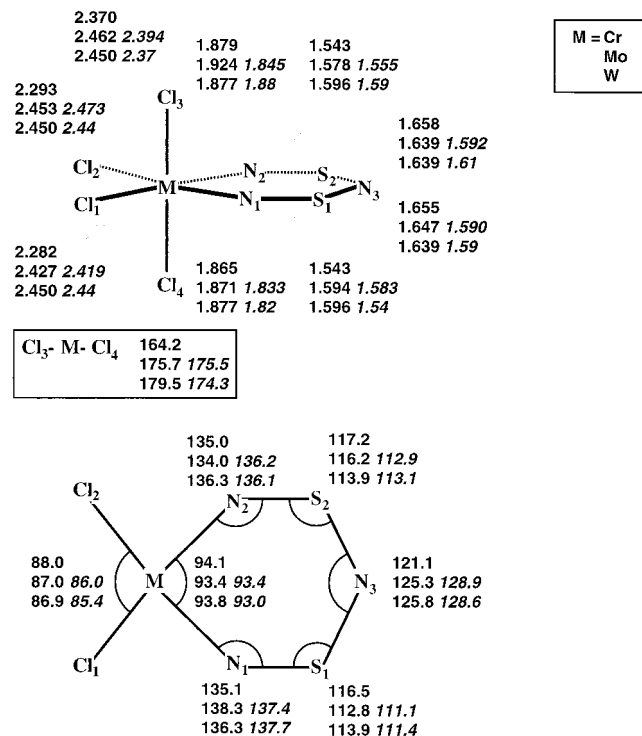


**Figure 16.** Optimized structural parameters for metallacyclothiazenes (in Å and deg; calculated at the B3LYP/SBK(d + diff) level). Experimental data<sup>18,19</sup> are given in italics.

There is a good agreement between calculated and experimental data. An analysis shows that the calculation has a systematical error in predicting the bond lengths; they result about 0.04 Å too long as compared with experiment. To explain this, one has to consider that on one hand the calculation deals with an isolated anion in the vacuum whereas in the experiment the results refer to a molecule in condensed matter. Another point is that anions are per se more difficult to describe by quantum chemical methods than neutral molecules or cations because the influence of electron correlation on bonding is larger, and this part of electron electron interaction is the most difficult one to model properly.

The optimized structures reflect the qualitative difference between the molybdenum and tungsten compound on the one hand and the chromium complex on the other hand. The N<sub>M</sub>-S bonds in the Cr complex are about 0.4 Å shorter than in the complexes of the higher homologues Mo and W. The N<sub>S</sub>-S bonds are 0.2 Å longer. This is in line with the Lewis structure C (Chart 5).

The simulated IR spectra are also in good agreement with experimental results (see Figure 17). Again, the spectra of the molybdenum and tungsten complex are similar. The spectrum of the chromium complex differs mainly in a band at 817 cm<sup>-1</sup> (N-S stretch). In the cases M = Mo and W this band is found with low intensity at 782 and 768 cm<sup>-1</sup>, respectively. This is another hint for the stronger N-S bonds in the chromium complex.

## 5. Conclusions

The results of our computational study can be summarized as follows: (1) The molecular structure and the vibrational spectra of metallacyclophosphazenes and -thiazenes are well reproduced by calculations at DFT level. (2) An analysis of the calculated electron density distribution reveals that the phos-

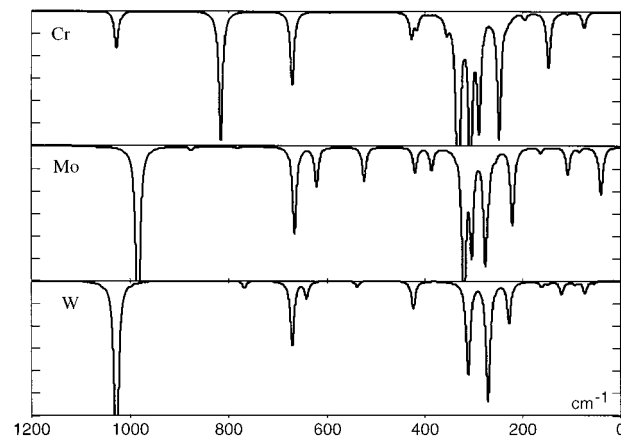


**Figure 17.** Simulated IR spectra for metallacyclothiazenes (calculated at the B3LYP/SBK(d + diff) level). The harmonic frequencies and intensities are superimposed with Lorentzians of half-width 10 cm<sup>-1</sup>. Intensities are scaled to the most intense band. Experimentally determined bands: Mo, 968 cm<sup>-1</sup> (calcd, 985 cm<sup>-1</sup>); W, 1011 cm<sup>-1</sup> (calcd, 1028 cm<sup>-1</sup>).

phazene and the thiazene ligand act as  $\sigma$  and  $\pi$  donors toward a transition metal atom. (3) The double bond character of the transition metal nitrogen bond is much less pronounced than in nitrido or imido complexes of the corresponding transition metal atoms. (4) There is some tendency to form localized double bonds as has been observed already for cyclic nitrido complexes, but the alternation of bond lengths in the ring is smaller. For metallacyclophosphazenes and -thiazenes fluctuating structures have to be expected. (5) Our calculations predict the existence of a dimetalla derivative of cyclophosphazenes, which should be an interesting target for experimental research.

## 6. Methodology

All molecules are fully optimized at B3LYP<sup>25</sup> level utilizing the effective core potential basis sets of Stevens, Basch, and Krauss,<sup>26,27</sup> augmented by one set of polarization functions (of d type) for the heavy (non-hydrogen) main group elements (SBK(d) basis). The use of polarization functions is imperative to get a correct description of the strongly polar N-P bond. For all anions this basis set is augmented by a set of diffuse s and p functions (SBK(d + diff)), to account for the larger extent of delocalization of the MOs in these molecules. To save CPU time, if possible symmetry constraints were used. All stationary points were characterized as local minima/transition states

- (25) Becke, A. D. *J. Chem. Phys.* **1993**, *98*, 5648–5653.  
 (26) Stevens, W. J.; Basch, H.; Krauss, M. *J. Chem. Phys.* **1984**, *81*, 6026–6033.  
 (27) Stevens, W. J.; Krauss, M.; Basch, H.; Jasien, P. G. *Can. J. Chem.* **1992**, *70*, 612–630.  
 (28) Reed, A. E.; Weinstock, R. B.; Weinhold, F. *J. Chem. Phys.* **1985**, *83*, 735–746.  
 (29) Frisch, M. J.; Trucks, G. W.; Schlegel, H. B.; Scuseria, G. E.; Robb, M. A.; Cheeseman, J. R.; Zakrzewski, V. G.; Montgomery, J. A., Jr.; Stratmann, R. E.; Burant, J. C.; Dapprich, S.; Millam, J. M.; Daniels, A. D.; Kudin, K. N.; Strain, M. C.; Farkas, O.; Tomasi, J.; Barone, V.; Cossi, M.; Cammi, R.; Mennucci, B.; Pomelli, C.; Adamo, C.; Clifford, S.; Ochterski, J.; Petersson, G. A.; Ayala, P. Y.; Cui, Q.; Morokuma, K.; Malick, D. K.; Rabuck, A. D.; Raghavachari, K.; Foresman, J. B.; Cioslowski, J.; Ortiz, J. V.; Stefanov, B. B.; Liu, G.; Liashenko, A.; Piskorz, P.; Komaromi, I.; Gomperts, R.; Martin, R. L.; Fox, D. J.; Keith, T.; Al-Laham, M. A.; Peng, C. Y.; Nanayakkara, A.; Gonzalez, C.; Challacombe, M.; Gill, P. M. W.; Johnson, B.; Chen, W.; Wong, M. W.; Andres, J. L.; Gonzalez, C.; Head-Gordon, M.; Replogle, E. S.; Pople, J. A. *Gaussian 98, Revision A.3*; Gaussian, Inc.: Pittsburgh, PA, 1998.  
 (30) Landrum, G. A. *YAeHMOP-Hückel Molecular Orbital Package, Version 2.0*. URL: <http://overlap.chem.cornell.edu:8080/yaehmop.html> (Cornell University, 1997).

by inspection of the eigenvalues of the corresponding Hessian matrixes (calculated at the DFT level, too). For population analyses the NBO partitioning scheme<sup>7,28</sup> was utilized. All calculations were performed using the Gaussian 98 package of programs.<sup>29</sup> For EHT calculations we used the program YAeHMOP.<sup>30</sup>

**Acknowledgment.** This work has been supported by the Deutsche Forschungsgemeinschaft and the Fonds der Chemischen Industrie.

IC990956E